Lab on a Chip

PAPER

View Article Online
View Journal | View Issue

Cite this: *Lab Chip*, 2015, **15**, 3934

Rapid, targeted and culture-free viral infectivity assay in drop-based microfluidics†

Ye Tao,‡[ab] Assaf Rotem,‡[a] Huidan Zhang,‡[ac] Connie B. Chang,[ad] Anindita Basu,[ae] Abimbola O. Kolawole,[f] Stephan A. Koehler,[a] Yukun Ren,[b] Jeffrey S. Lin,[g] James M. Pipas,[h] Andrew B. Feldman,[g] Christiane E. Wobus[f] and David A. Weitz*[ai]

Received 17th May 2015,
Accepted 14th August 2015

DOI: 10.1039/c5lc00556f

www.rsc.org/loc

A key viral property is infectivity, and its accurate measurement is crucial for the understanding of viral evolution, disease and treatment. Currently viral infectivity is measured using plaque assays, which involve prolonged culturing of host cells, and whose measurement is unable to differentiate between specific strains and is prone to low number fluctuation. We developed a rapid, targeted and culture-free infectivity assay using high-throughput drop-based microfluidics. Single infectious viruses are incubated in a large number of picoliter drops with host cells for one viral replication cycle followed by in-drop gene-specific amplification to detect infection events. Using murine noroviruses (MNV) as a model system, we measure their infectivity and determine the efficacy of a neutralizing antibody for different variants of MNV. Our results are comparable to traditional plaque-based assays and plaque reduction neutralization tests. However, the fast, low-cost, highly accurate genomic-based assay promises to be a superior method for drug screening and isolation of resistant viral strains. Moreover our technique can be adapted to measuring the infectivity of other pathogens, such as bacteria and fungi.

Introduction

Viruses are the most abundant, rapidly evolving and diverse biological entities, and are responsible for numerous infectious disease. The underlining causes for viral outbreaks are their fast infectivity evolution. Recent examples of viral epidemics range from the common cold to AIDS, as well as recent Ebola outbreaks in West Africa.[1–3] The gold standard for detecting infectious viruses is the plaque assay. In such assays, viruses are inoculated onto monolayers of susceptible host cells, and after incubation periods extending up to several weeks, infectious particles produce visible circular zones of infected cells called plaques. The titer of a virus stock is calculated in plaque-forming units (PFU) per milliliter.[4,5] However, plaque assays are time-consuming and require virus-specific host cells, which in case of unculturable viruses are not unavailable.[6] Moreover, since the specificity of plaque-based assays depends upon host cells, studies involving viral mutants or host cells susceptible to a range of pathogens require either tedious sample purification or cumbersome identification of the plaques.[7] In comparison, real-time quantitative PCR (qPCR) techniques offer a fast and targeted measurement of viral concentration based on genomic content. Nevertheless, qPCR is unable to precisely measure infectivity because the number of particles doesn't correlate directly with the number of infections.[8,9] Therefore, assays that can provide timely information about viral infectivity are still missing. Establishing such assays will dramatically accelerate viral study, thereby enabling quicker therapeutic decisions as well as decreasing the development time for vaccines and antiviral drugs.

[a] *School of Engineering and Applied Sciences, Harvard University, Cambridge, MA 02138, USA*
[b] *School of Mechatronics Engineering, Harbin Institute of Technology, Harbin 150001, China*
[c] *Department of Cell Biology, Key Laboratory of Cell Biology, Ministry of Public Health, and Key Laboratory of Medical Cell Biology, Ministry of Education, China Medical University, Shenyang 110001, China*
[d] *Chemical and Biological Engineering Department, Montana State University, Bozeman, MT 59717, USA*
[e] *Broad Institute of MIT and Harvard 7 Cambridge Center, MA 02142, USA*
[f] *Department of Microbiology and Immunology, University of Michigan, Ann Arbor, MI 48109, USA*
[g] *Applied Physics Laboratory, Johns Hopkins University, Laurel, Maryland 11100, USA*
[h] *Department of Biological Sciences, University of Pittsburgh, Pittsburgh, PA 15260, USA*
[i] *Department of Physics, Harvard University, Cambridge, MA 02138, USA. E-mail: weitz@seas.harvard.edu*

† Electronic supplementary information (ESI) available: PDF file provides sensitivity analysis of Drop-based infectivity measurements. ZIP file provides the DetectionAnalysis.m and DetectionAnalysis.fig Matlab GUI code for analyzing text files recording drop size and fluorescence, and an example of a text file recorded from reading drops. Movie S1 shows encapsulation of cells. Movie S2 shows drop reinjection. Movie S3 shows spacing of drops. Movie S4 shows drop splitting and pico-injection. DOI: 10.1039/c5lc00556f

‡ These authors contributed equally to this work.

Micron size drops containing both viruses and their hosts have been used previously as microenvironments for the replication of viruses.[11] Building on these capabilities we develop a drop-based culture-free microfluidic method for rapid and targeted detection of viral infectivity by combining the advantages of plaque-based assay and qPCR. We co-encapsulate single infectious viruses with host cells into a large number of picoliter-sized drops and incubate them for the duration of one viral replication cycle. The drops are then combined with a gene-specific PCR cocktail that fluoresces in the presence of replicated target viruses, and quantified using a custom-built high-throughput drop reader to determine the number of viral infections. The experimental design is illustrated in Fig. 1A. We compare our results with the conventional plaque-based infectivity assay and further demonstrate the utility of this technique by determining the effectiveness of a viral neutralizing antibody.

Results and discussion

The first step in our method for detecting infectious viruses is to generate uniform individual virus-cell infection compartments. We use a suspension of MNV-1 viruses whose concentration of 10^8 PFU per mL was measured by viral plaque assay.[10] The average Burst Size of MNV is B_s ~ 10 000 viral genomes per successful infection; however, only a small fraction of the progeny are actually infectious and the ratio of viral genomes to PFU is R_g ~ 100.[11] We use a microfluidic drop-maker to co-encapsulate murine norovirus strain MNV-1 and murine macrophage RAW cells into 100 μm mono-dispersed drops, as shown in Fig. 1B and Movie S1.† Viruses and cells are fed into the drop-making device from separate inlets so that they only come in contact inside the drop. Drops are formed at a rate of 2000 drops per second, thereby generating a million compartments in 10 min for high-throughput screening. We dilute the cell suspension so that on average each drop is occupied by 1–2 cells and find that 86% of drops contain one or more cells, as shown in Fig. 1C, 2A and Movie S1.†

To test the accuracy of our method we used a suspension of MNV-1 viruses at a concentration of 10^8 PFU per mL as measured by viral plaque assay.[10] By diluting the suspension we co-encapsulate the viruses together with RAW cells in drops at viral concentrations ranging from an average of 1 virus per drop to 0.001 virus per drop, or one virus in every 1000 drops. We collect the drops and incubate them for 24 hours allowing the viruses to complete one replication cycle.[12,13] Each infectious MNV typically produces 10 000 viral genomes during replication.[11]

To detect a successful infection we amplify the target viral genomes inside each drop using reverse transcription (RT) of the viral RNA genome followed by PCR. Since viral genomes are encapsulated within protein capsids, we must release the viral RNA prior to in-drop RT-PCR by heat-shocking the incubated drops. We then add a solution containing RT-PCR cocktail into each drop, utilizing a microfluidic-based pico-injection technique.[14] Unfortunately, when the RT-PCR is injected directly to the incubated drops, we couldn't obtain efficient amplification of viral genomes, possibly due to PCR inhibitors present in the host cells. In contrast to conventional RT-PCR assays that include a washing step to purify RNA, one challenge in drop-based assays is the inability to wash the contents of drops.

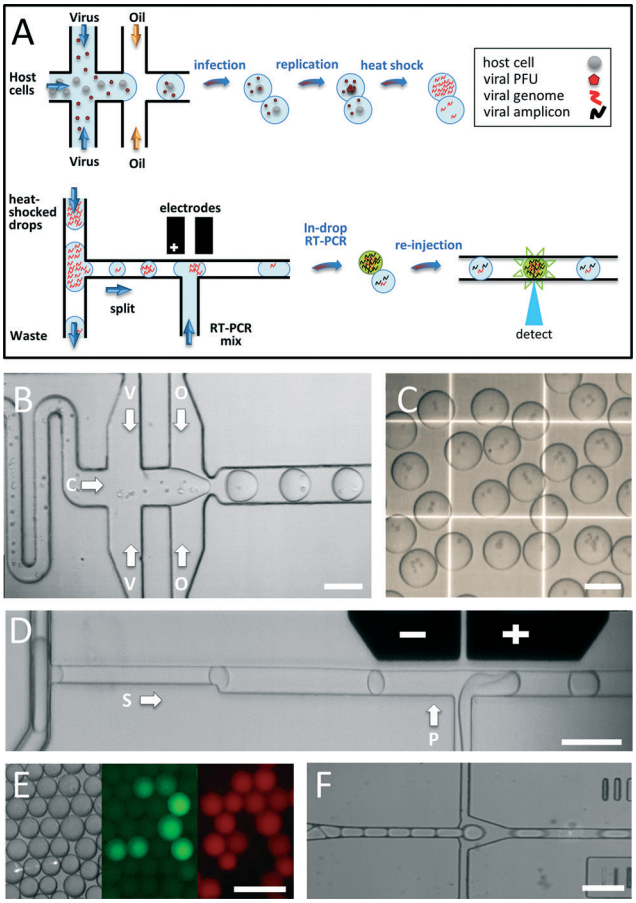

Fig. 1 Workflow of the drop-based viral infectivity assay. A) Schematic description of the assay. Viruses that infect host cells within drops produce many copies of their genome so that when fractions of these drops are merged with RT-PCR mix and amplified, many amplicons of the viral genome are produced and their marker fluoresce is at high intensity. By contrast, in drops where no infection occurred, very few viral templates if at all exist in the fractions of the original drops and the number of amplicons generated after a limited number of PCR cycles is significantly lower, as is the fluorescence of their marker. B) Viruses (V) and host cells (C) are co-encapsulated in oil (O) using a microfluidic drop-making device. C) An image of the resulting drops showing that each contain about 1–2 cells. D) After incubation, drops are re-injected into the "split and inject" device, where a small volume is split (S) from each drop and merged using electro-coalescence with RT-PCR mix (P). E) After off-chip in-drop amplification the drops remain monodisperse (left), those containing viral amplicons fluoresce at 520 nm (middle) and those containing tracer Rhodamine fluorescence at 586 nm (right). F) The drops are re-injected into a microfluidic drop reader device with a laser and a Photo-Multiplier (PMT) aligned to the channel for the detection of drop fluorescence. All scale bars are 100 μm.

To decrease the amount of cellular inhibitors in the drops prior to amplification we can dilute the contents of the drop. Typically, to dilute the contents of drops, more medium is added to each drop, but increasing drop size decreases the

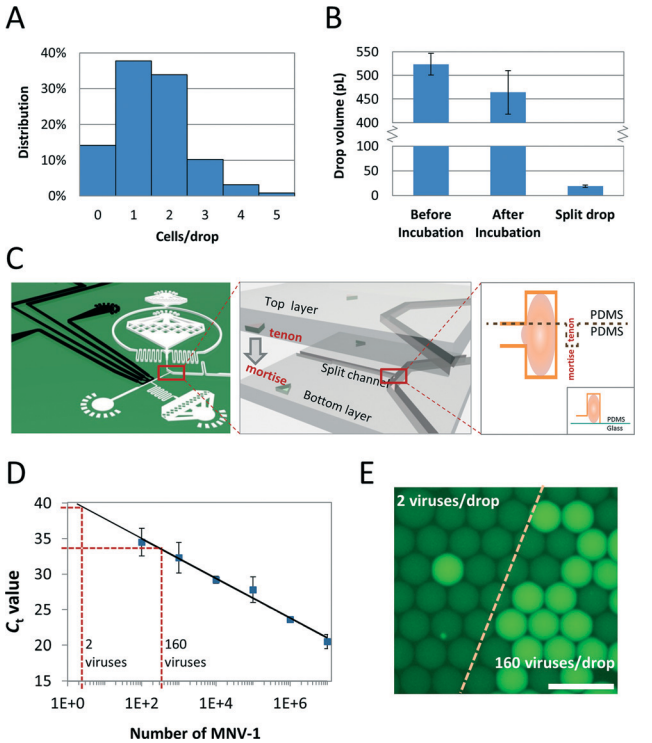

Fig. 2 Development of the viral infectivity assay. A) Distribution of the number of cells per drop, as measured from N = 127 drops before incubation. B) Average drop volume before incubation, after incubation and after splitting. Volumes were calculated from images as described in the methods. C) Design of the 3D multi-layered microfluidic "split and inject" device. Left: Schematic of the microfluidics showing the special structure and assembly of the two parts of the device to achieve the vertically centred split channel. Right: Vertical cross-section of the split junction. Top diagram shows the location of a drop in the vertically centred channel, enabling the split, while bottom diagram demonstrates the case of a non-vertically centred junction, where only oil flows into the split channel. D) Bulk real-time RT-PCR of a dilution series of the viral sample. C_t value, the number of PCR cycles required to amplify a template above a threshold concentration value is plotted *vs.* number of viruses in the sample. E) Fluorescence image of drop samples containing 2 viruses per drop (left) or 160 viruses per drop (right) after 32 cycles of RT-PCR amplification. The dash line separates between the two samples. The scale bar is 100 μm.

thermal stability of the drops and increases coalescence rate during PCR thermocycling. To overcome these problems, we design a microfluidic "split and inject" device that removes most cellular RNA and debris by sampling a small fraction of the incubated drops and then fusing it with the RT-PCR mix, as shown in Fig. 1D and Movie S4.† The extremely asymmetric splitting ratio is difficult to obtain in single-layered microfluidic devices[15] or in multi-layered devices with vertically asymmetric profiles (see Fig. 2C), and requires a specially designed PDMS–PDMS non-planar so called "3D" device, with a split channel whose height is smaller than the main channel and which is vertically centred with respect to it (see Methods).[16] 98% of drops split in our device, at a ratio of 1/64 ± 15%, as shown in Movie S4† and Fig. 2B. The "split and inject" device operates at a rate of ~250 drops per second and we typically process ~100 000 incubated drops from each sample.

To inject RT-PCR cocktail into every drop, we keep the flow rate of RT-PCR mix higher than is required for injection into the split drops (Movie S4†). As a result, all the split drops are injected with RT-PCR mix but the injection junction also generates drops that only contain the RT-PCR mix. These so called "empty drops", which constitute 63% of all drops, can introduce a large number of false negative if counted as unsuccessful infections at the detection stage, thus distorting the final infectivity measurement. To overcome this problem and to further verify the rate of "empty drops", we add Rhodamine B into the RAW cell suspension before co-encapsulation with viruses. Rhodamine B was found to be inert with regard to our assay and is used to separate infectivity assay bearing drops from "empty drops".

The background of viral genomes from the encapsulation step increases the risk for false positive detection of unsuccessful infections because there are still some viral RNA genomes from the original loading even if no replication has occurred. When loading viruses at 1 PFU per drop, each drop contains about a background level of R_g ~ 100 viral genomes.[12] In the case of unsuccessful infection, even after splitting 1/64 of the drop component, one or two of the parental viruses are expected to partition into the split drops. Since RT-PCR is capable of amplifying a single copy of viral RNA,[17] we need to optimize the number of thermocycles used to distinguish between background viral load and true infection events. Drops with successful infection, are expected to contain about 10 000 viral genomes,[11] so that ~160 viruses partition into the split drop. Using quantitative RT-PCR with a serial dilution of viruses, we first determine an approximate range for the number of cycles required to amplify as shown in Fig. 2D. Based on these approximations, we perform in-drop RT-PCR amplification of 2 genomes per drop and of 160 genomes per drop with a range of cycle numbers and find that 32 cycles are optimal for distinguishing between the two concentrations, as shown in Fig. 2E.

To validate our method, we first compare the concentration of our stock solution (10^8 PFU per mL) to our in-drop assay of viral infectivity applied on a dilution series of the stock. After adding our MNV-1 specific RT-PCR cocktail into every split drops, drops are thermocycled off-chip, and re-injected into a microfluidic drop fluorescence reader (Fig. 1F) to quantify the number of infectious viruses. Successful in-drop infection is indicated by significantly increased green fluorescence signal (520 nm), from the hydrolysis of the MNV-1 specific FAM-labelled Taqman probe in the RT-PCR cocktail. Red fluorescence (586 nm) marks the presence of Rhodamine B in the drops, indicating that they contain a fraction of the original infection assay (Fig. 1E). When the red and green fluorescence intensities of each drop are plotted in a 2D distribution plot, they cluster in 3 quadrants as shown in the left panel of Fig. 3A. Drops clustered in the quadrant 1 only fluoresce in green. These are "empty drops" that only contain RT-PCR mix. Quadrant 1 contains 65% of

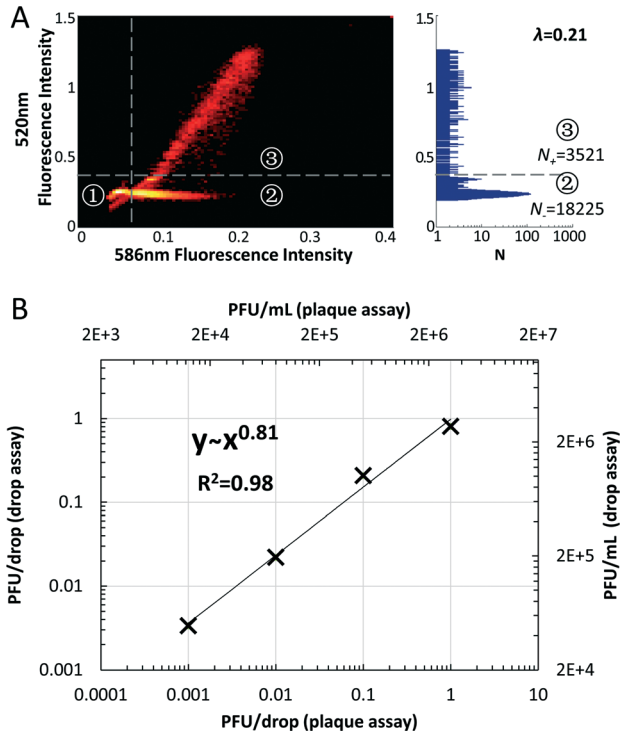

Fig. 3 Quantification of the MNV-1 stock. A) Heat map of the mutual distribution of fluorescence of 35 000 drops in the two wavelengths (520 nm, *y*-axis and 586 nm, *x*-axis) and a histogram of the fluorescence at 520 nm of drops containing on average 0.1 PFU. Graphs were produced by an interactive Matlab code, see Methods. B) The PFU per mL calculated for each serial dilution experiment plotted *vs.* the dilution factor in each experiment.

all drops, which is consistent with the observations from Movie S4† where 63% of drops only contain the RT-PCR cocktail. Since the fraction of "empty drops" was consistent across all dilution experiments, we concluded that there was no need to add Rhodamine when performing a comparative experiment such as a neutralizing assay; drops clustered in the second region (quadrant 2) fluoresce at the same green level as the drops clustered in quadrant 1, but at higher red level, representing drops containing the original infectivity assay where viral replication was not successful; finally, drops that fluoresce in both red and green (quadrant 3) represent successful replication of viruses.

To determine the concentration of infectious viruses we analyse the number of true negatives or dark drops (N_-) in quadrant 2 and true positives or bright drops (N_+) in quadrants 3 shown in the right panel of Fig. 3A, using Poisson statistics. In our context, the Poisson distribution describes how many infectious viruses, k, are contained within a sample taken from the viral solution, $P(k) = e^{-\lambda}(\lambda^k/k!)$, where the Poisson parameter $\lambda = CV$ is the average number of infectious particles expected per drop with volume V and PFU concentration C. The probability of true positives (N_+/N_{total}) in which a drop harbours an infection event is $P(k > 0) = 1 - e^{-\lambda}$. Solving for the Poisson parameter in terms of the total number of drops and the number of negative drops gives $\lambda = \log(N_{total}/N_-)$, which can be converted to PFU per mL upon division by the drop volume. Since only 86% of the co-encapsulated drops contain cells, the corrected total number of cell-loaded and thus valid drops is $N_{total} = 0.86(N_+ + N_-)$. For small PFU concentrations, the accuracy of λ increases with the square root of the number of bright drops. To show this, we use the Poisson noise for detecting positive events: $\sigma(N)/N \sim 1/\sqrt{N}$. In the limit of small λ, $\lambda \approx N_+/N_{total}$ and its error can be estimated by error propagation as:

$$\frac{\sigma(\lambda)}{\lambda} = \sqrt{\left(\frac{\sigma(N_+)}{N_+}\right)^2 + \left(\frac{\sigma(N_{total})}{N_{total}}\right)^2} \sim \frac{\sigma(N_+)}{N_+} \sim \frac{1}{\sqrt{N_+}}$$

For example, 100 positive drops are sufficient for measuring λ at an accuracy of ~10%, which, for a sample of 0.001 PFU per drop means detecting 100 000 drops. We fit the data from the dilution series and obtain a slightly sublinear relationship between the measured infectivity and the PFU concentration, where the exponent is 0.81 and the coefficient of determination (R^2) is 0.98 as shown in Fig. 3B. Averaged across all four trials our measured infectivity is 2.2 ± 1.0 times that of the plaque assay. Considering the measurement uncertainties and that infectivity measurements span several orders of magnitude, our values are in good agreement with plaque assay measurements and thereby validate our method.

Our drop-based assay can be modified for other viral species based upon two critical properties of the virus: the burst size, B_s, and the ratio of viral genomes to PFU, R_g. The burst size limits the splitting ratio of the drops, f; we recommend for consistent Poisson loading that on average at least ten genomes from each infected drop are in the split-off volume: $f \geq 10/B_s$. For example, our current sampling setting $f = 1/64$ is inadequate for viruses with a low burst size of $B_s = 100$ and will result in low loadings of progeny in the split-off drop and a 20% chance that no genomes are sampled. Altering the splitting ratio in our device is possible either by changing the flow rates or, for larger changes, modifying the geometry of the splitting junction. The ratio B_s/R_g limits the range of detectible Poisson loading of drops, because to successfully identify infections the number of genomes resulting from an infection has to be significantly larger than the number of background genomes, $B_s \gg \lambda \cdot R_g$. Therefore the upper limit on the detectable concentrations is $\lambda \ll B_s/R_g$. Another important optimization parameter is the number of PCR cycles, N, necessary to create fluorescence suitable for optical detection. This number depends on the number of genomes that are sampled from infected drops, $f \cdot B_s$, and the maximum number of genomes sampled in a non-infected drop, which regardless of dilution is at least one. To distinguish between these two types of events, the dynamic range of N is

$$\Delta N = \log_2(f \cdot B_s) - \log_2(\max\{\lambda \cdot R_g, 1\}).$$

In the limit of small concentrations and for $f \cdot B_s \sim 100$, the dynamic range is about $\Delta N \sim 7$, whereas for $f \cdot B_s \sim 10$ the

dynamic range drops to about $\Delta N \sim 3$. These analyses are illustrated in Fig. S1.†

To further demonstrate the utility of our drop-based technique for viral studies, we perform a plaque reduction neutralization test. We mix six MNV-1 variants[18] with either a neutralizing antibody MAb A6.2 (Ab), or a negative control isotype that has no effect. The neutralization rate is defined as the reduction in replication rate in the presence of Ab compared to the replication rate in the presence of the isotype. We measure the infectivity for all six variants in the presence of Ab and in the presence of the isotype and register the ratio between the two replication rates. The results of our infectivity test in the presence of Ab is given for one of the variants, 378A that is neutralized by a factor of 4, as shown in Fig. 4A. We summarize the results from all 6 variants (see Methods) and compare them to results obtained from traditional plaque reduction neutralization assay. The results from both experiments agree well with each other (Pearson correlation of 0.93), as shown in Fig. 4B.

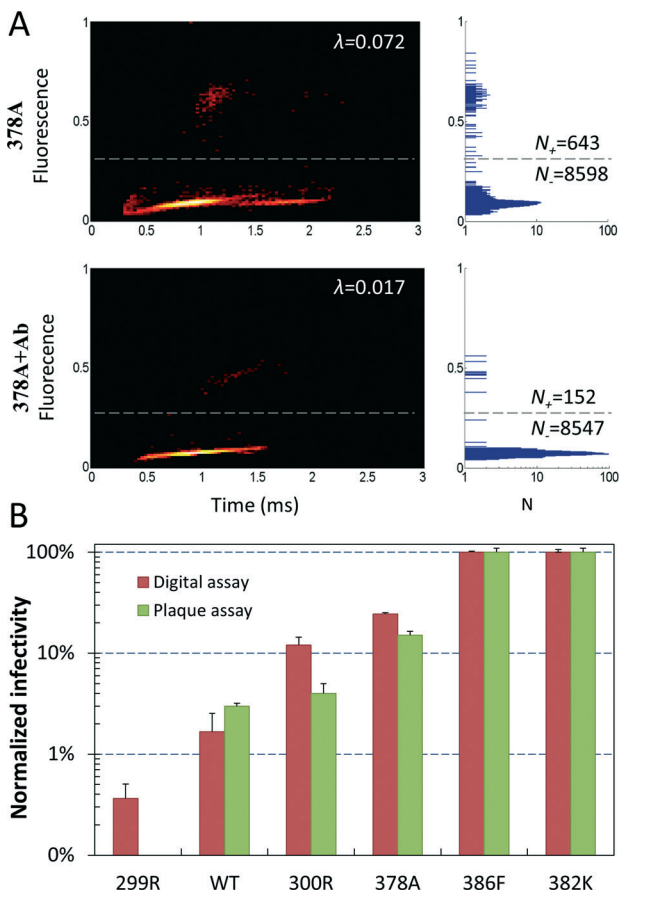

Fig. 4 In-drop neutralization test. A) The heat map and histograms of the infectivity test of 378A MNV-1 variant. Infected drops are clustered above the threshold (horizontal dashed line). The neutralization rate is calculated as the ratio between the measured concentration of PFUs without antibody (top) and that measured in the presence of antibody (bottom). B) The neutralization rate of six MNV-1 variants by antibody as measured by our in-drop viral infectivity assay (digital assay) and by conventional plaque reduction test (plaque assay).

Conclusions

Here we developed a new viral infectivity assay using drop-based microfluidics. Replication within picoliter bioreactors[11] combined with in-drop detection of viral genomes enables the reliable detection of a single infection event. Thus, our test requires just a single replication cycle, significantly less than the multiple generations required for forming a viral plaque in the conventional assay. Moreover, this also potentially eliminates the need for culturing the host cells, enabling culture-free detection of infectious viruses. This will allow detecting viral infectivity from primary cells and quickly determine host cells that are susceptible to certain viruses. The high throughput detection of our microfluidics system enables us to measure extremely rare infection events thus providing a large dynamic range for any single experiments and alleviates the need for serial dilution experiments. Finally, the integration of a target specific RT-PCR amplification in the infection assay renders our method highly specific to viral species or even viral genes within a species.

Notwithstanding the advantages of our novel method, differences in culturing and incubation between plaque and drop-based assays may affect the infectivity measurements. In drop-based assays, host cells adapt to non-adherent conditions, which may change their susceptibility to viral infections. Additionally, viruses and cells co-encapsulated in a single drop have an increased probability of colliding compared to plaque assays where viruses collide with a monolayer of cells.[19] Plaque assays allow only a short incubation time for the attachment of PFU to cells before washing the remaining particles away whereas in our drop-based assay cells are exposed to all particles throughout the experiment.[10] Finally, the large surface to volume ratio in drop-based assays may increase the absorption of particles to the drop interface. These factors have the potential to bias measurements, possibly explaining the slightly larger values of MNV-1 infectivity measured in drops. However in many cases, such as neutralization tests, relative rather than absolute values of the infectivity are required. Moreover, plaque and drop-based assays are both *in vitro* measurements, and their correlation with *in vivo* measurements has to be studied to better evaluate their respective biases.

In the future, our method can be combined with microfluidic drop sorting[20] to isolate viruses that resist antiviral treatment and sequence their genome to study the mutations driving the escape.[21] Moreover, our microfluidic platform could be adapted to detect the infectivity, drug resistance and heterogeneity of bacteria,[22,23] specifically intracellular parasites that replicate within human host cells such as *Listeria*, *Salmonella* and *Legionella*.[24,25] Thus, drop-based infectivity assays may potentially revolutionize measurement of infectious titers of a variety of pathogens.

Experimental procedures

Cells and viruses

We purchase murine macrophages RAW 264.7 cells from ATCC and maintain them as described previously.[13,26] Cells

are adapted to culture in suspension for drop encapsulation experiments.[11] The plaque-purified MNV-1 clone (GV/MNV1/2002/USA) MNV-1.CW3 (referred to herein as MNV-1) is used at passage 6 (P6) for all experiments.[27] Five viral mutants, S299R, G300R, V378A, L386F and A382K, containing point mutations in the MNV-1 P domains were generated as described previously.[18] Some of these mutants are known to abrogate MAb A6.2 binding to MNV-1 and allow MAb A6.2 neutralization escape in culture.[18] Virus titers are determined by plaque assay as described in ref. 10.

Quantitative reverse transcriptase polymerase chain reaction (qRT-PCR)

The primers of a MNV-1 conserved fragment in ORF1 (nt 39-177) were purchased from Integrated DNA Tech, Fc: 5′-GTGCGCAACACAGAGAAACG-3′ and Rc: 5′-CGGGCTGA GCTTCCTGC-3′, respectively.[28] The Taqman probe, 5′-FAM/CTAGTGTCTCCTTTGGAGCACCTA/-MGB-3′, is synthesized by Life Tech based on the sequence reported before,[28] using a minor groove binder (MGB) as the quencher molecule. We perform a serial dilution of MNV-1 stock solution in volumes of 12.5 μL. We then use a 12.5 μL of 2× One-step RT-PCR cocktail for every sample, each containing 1 μL of Enzyme Mix with 2× buffer (Qiagen), 800 μM dNTPs, 1 μM forward and reverse primers, 1 μM Taqman probe, 0.8 μg μL^{-1} BSA, and 0.8% Tween 20. Quantitative RT-PCR is performed on an Applied Biosystems 7900HT real time PCR machine (Life Tech) using the following thermal cycling parameters: 30 min at 50 °C, 10 min at 95 °C, 40 cycles of 30 s at 95 °C, 30 s at 58 °C and 40 s at 72 °C.

Microfluidic device fabrication

We fabricate polydimethylsiloxane (PDMS) microfluidic devices using standard soft lithographic methods.[29] To make the "split and inject" device, we use a modified PDMS replica moulding protocol for 3D multiple layered devices.[16] We use a 25 μm thick centre layer and a thickness of 35 μm for the top and bottom layers. Thus, the main channel is 40 μm wide and 95 μm high, and the splitting channel is 25 μm wide and 25 μm high, and vertically centred with respect to the main channel. To induce electro-coalescence, electrodes are designed as channels in the PDMS device.[30] These channels are filled with Indalloy 19 (51% In, 32.5% Bi, 16.5% Sn; 0.020 inch diameter), a low melting-point metal alloy (Indium Corp.), by pushing the alloy wire into the punched holes on a 80 °C hot plate. Because all channel walls of the 3D device are PDMS, heating the alloy to 80 °C is challenging given the high thermal resistance of PDMS. Instead, the holes accessing the electrode channels are punched throughout the PDMS slab and then the device is bonded to a cover glass so that the alloy inserted into these holes makes contact with the heated glass and conducts heat throughout the channel.

Electrical connections are made to the on-chip electrodes using eight-pin terminal blocks (Phoenix Contact). We treat the microfluidics channel with Aquapel (PPG) to render them hydrophobic and to minimize absorption of viral particles.

Co-encapsulation and incubation

We use a co-flow drop maker with a cross section of 100 μm^2 to co-encapsulate cells at a concentration of 3.8×10^6 cells per mL, and viruses at varying concentrations into 100 μm monodisperse aqueous drops at a 1 : 1 ratio in HFE-7500 oil, (3M), containing 1% (w/w) Krytox-PEG diblock co-polymer surfactant (RAN Biotechnologies), as shown in Movie S1.† To test the neutralizing antibody, we mix 60 ng MAb A6.2 into 500 μL viral solution and incubated them for 30 min before infecting cells. Meanwhile, the cell suspension also contains 120 ng mL^{-1} MAb to keep the MAb concentration stable after drop making. We then inject the cell suspension and viral solution into two sample inlets of the co-flow drop maker, respectively. The drops are collected into a 15 mL falcon tube, and incubated for 24 hours at 37 °C. To break the viral capsid and release the viral genome for downstream RT-PCR, we heat the drops for 3 min at 90 °C. This heating process also releases the viruses trapped inside cells.

Viral genome sampling and injection of RT-PCR cocktail

In our device, a small microfluidic channel is utilized to split the original drops into two drops, with the smaller one continuing into the split channel and the bigger one flushed out through the waste channel. The drop splits unequally if the two daughter channels have different fluidic resistances. Since fluidic resistance is proportional to microchannel cross section area, according to the Hagen–Poiseuille equation, changing the area of one of the split channels allows drops to be split unevenly. In our experiment, the sampling volume of the daughter droplet produced by the fission can be measured to be $(4\pi(25/2)^3)/3000 = 8.2$ pL, with a fission ratio of 8.2/524 = 1.56%.

To perform the split and injection, we re-inject drops at 0.5 mL h^{-1}, space them with oil flowing at 4 mL h^{-1} and add the RT-PCR mix at a flow rate of 0.1 mL h^{-1}, spaced with an addition oil phase flowing at 0.2 mL h^{-1}. The injected 50 μL of RT-PCR cocktail contains 4 μL of Qiagen OneStep RT-PCR Enzyme Mix (Qiagen), 2× Qiagen OneStep RT-PCR buffer, 800 μM dNTPs, 0.5 μM of Fc and Rc, 0.5 μM Taqman probe, 0.4 μg μL^{-1} BSA and 1 μL 10% Tween 20. The drop-based RT-PCR is done in one step by combining RT and PCR reactions. The thermocycling condition is 50 °C for 30 min (RT), 95 °C for 10 min (initial denaturation and enzyme activation), 32 cycles of 95 °C for 30 s, 58 °C for 30 s, and 72 °C for 40 s, followed by a final extension at 72 °C for 5 min.

Detection of drop fluorescence

The thermocycled drops are re-injected into a microfluidic detection device at a flow rate of 15 μL h^{-1} and evenly spaced by using HFE-7500 oil without surfactant flowing at a rate of 180 μL h^{-1} in a 40 μm^2 cross-section channel for fluorescence detection.[20] When a drop passed by the laser spot, its

fluorescence was observed by a microscope objective and focused on a photomultiplier tube (Hamamatsu), connected to a real-time field-programmable gate array card (National Instruments) controlled using LabView (National Instruments). Each drop had an intrinsic fluorescence signal from the incomplete quenching of the fluorogenic probes, enabling the detection of every drop, including those containing no amplified template (dark drops).

Calculation of drop volume

To determine the volume fraction that is split from the drops that are injected into the "split and inject" device, we calculate the volume of drops based on the following formula:[31]

$$V = \left[HW - (4-\pi)\left(\frac{2}{H}+\frac{2}{W}\right)^{-2} \right]\left(L-\frac{W}{3}\right)$$

where H is the channel height, W is the channel width, and L is the droplet length.

Data analysis

The fluorescence of each drop is registered by a custom LabView code and saved for offline analysis. A custom MatLab interactive program is used to load the raw files and analyse them to produce the final counts for each sample.

Acknowledgements

This work was supported by Defence Advanced Research Projects Agency (DARPA) grant HR0011-11-C-0093 and National Natural Science Foundation of China (Grant No. 81372496). This work was performed in part at the Center for Nanoscale Systems (CNS) at Harvard University, a member of the National Nanotechnology Infrastructure Network (NNIN), which is supported by the National Science Foundation under NSF Award ECS-0335765.

References

1 J. A. Al-Tawfiq, A. Zumla, P. Gautret, G. C. Gray, D. S. Hui, A. A. Al-Rabeeah and Z. A. Memish, *Lancet Infect. Dis.*, 2014, **14**, 992–1000.
2 G. Maartens, C. Celum and S. R. Lewin, *Lancet*, 2014, **384**, 258–271.
3 D. Gatherer, *J. Gen. Virol.*, 2014, **95**, 1619–1624.
4 I. A. Hamza, L. Jurzik, K. Uberla and M. Wilhelm, *Int. J. Hyg. Environ. Health*, 2011, **214**, 424–436.
5 A. Maeda and J. Maeda, *Vet. J.*, 2013, **195**, 33–40.
6 Y. Kamimura and L. L. Lanier, *J. Virol. Methods*, 2014, **205C**, 53–56.
7 E. Mathijs, B. Muylkens, A. Mauroy, D. Ziant, T. Delwiche and E. Thiry, *J. Gen. Virol.*, 2010, **91**, 2723–2733.
8 R. M. Ratcliff, G. Chang, T. Kok and T. P. Sloots, *Curr. Issues Mol. Biol.*, 2007, **9**, 87–102.
9 R. A. Rodriguez, I. L. Pepper and C. P. Gerba, *Appl. Environ. Microbiol.*, 2009, **75**, 297–307.
10 M. B. Gonzalez-Hernandez, J. Bragazzi Cunha and C. E. Wobus, *J. Visualized Exp.*, 2012, e4297, DOI: 10.3791/4297.
11 A. E. Fischer, S. K. Wu, J. B. Proescher, A. Rotem, C. B. Chang, H. Zhang, Y. Tao, T. S. Mehoke, P. M. Thielen, A. O. Kolawole, T. J. Smith, C. E. Wobus, D. A. Weitz, J. S. Lin, A. B. Feldman and J. T. Wolfe, *J. Virol. Methods*, 2015, **213**, 111–117.
12 M. Asanaka, R. L. Atmar, V. Ruvolo, S. E. Crawford, F. H. Neill and M. K. Estes, *Proc. Natl. Acad. Sci. U. S. A.*, 2005, **102**, 10327–10332.
13 C. E. Wobus, S. M. Karst, L. B. Thackray, K. O. Chang, S. V. Sosnovtsev, G. Belliot, A. Krug, J. M. Mackenzie, K. Y. Green and H. W. Virgin, *PLoS Biol.*, 2004, **2**, e432.
14 A. R. Abate, T. Hung, P. Mary, J. J. Agresti and D. A. Weitz, *Proc. Natl. Acad. Sci. U. S. A.*, 2010, **107**, 19163–19166.
15 D. R. Link, S. L. Anna, D. A. Weitz and H. A. Stone, *Phys. Rev. Lett.*, 2004, **92**, 054503.
16 A. Rotem, A. R. Abate, A. S. Utada, V. van Steijn and D. A. Weitz, *Lab Chip*, 2012, **12**, 4263–4268.
17 R. A. White 3rd, S. R. Quake and K. Curr, *J. Virol. Methods*, 2012, **179**, 45–50.
18 A. O. Kolawole, M. Li, C. Xia, A. E. Fischer, N. S. Giacobbi, C. M. Rippinger, J. B. Proescher, S. K. Wu, S. L. Bessling, M. Gamez, C. Yu, R. Zhang, T. S. Mehoke, J. M. Pipas, J. T. Wolfe, J. S. Lin, A. B. Feldman, T. J. Smith and C. E. Wobus, *J. Virol.*, 2014, **88**, 4543–4557.
19 T. T. Puck, A. Garen and J. Cline, *J. Exp. Med.*, 1951, **93**, 65–88.
20 J. J. Agresti, E. Antipov, A. R. Abate, K. Ahn, A. C. Rowat, J. C. Baret, M. Marquez, A. M. Klibanov, A. D. Griffiths and D. A. Weitz, *Proc. Natl. Acad. Sci. U. S. A.*, 2010, **107**, 4004–4009.
21 M. Tan, R. S. Hegde and X. Jiang, *J. Virol.*, 2004, **78**, 6233–6242.
22 O. Gefen and N. Q. Balaban, *FEMS Microbiol. Rev.*, 2009, **33**, 704–717.
23 L. A. Magdanova and N. V. Goliasnaia, *Mikrobiologiia*, 2013, **82**, 3–13.
24 K. Ireton, L. A. Rigano, L. Polle and W. D. Schubert, *Front. Cell. Infect. Microbiol.*, 2014, **4**, 21.
25 A. M. Richards, J. E. von Dwingelo, C. T. Price and Y. Abu Kwaik, *Virulence*, 2013, **4**, 307–314.
26 S. Taube, J. R. Rubin, U. Katpally, T. J. Smith, A. Kendall, J. A. Stuckey and C. E. Wobus, *J. Virol.*, 2010, **84**, 5695–5705.
27 S. Taube, J. W. Perry, E. McGreevy, K. Yetming, C. Perkins, K. Henderson and C. E. Wobus, *J. Virol.*, 2012, **86**, 5584–5593.
28 S. Taube, J. W. Perry, K. Yetming, S. P. Patel, H. Auble, L. Shu, H. F. Nawar, C. H. Lee, T. D. Connell, J. A. Shayman and C. E. Wobus, *J. Virol.*, 2009, **83**, 4092–4101.
29 J. C. McDonald, D. C. Duffy, J. R. Anderson, D. T. Chiu, H. Wu, O. J. Schueller and G. M. Whitesides, *Electrophoresis*, 2000, **21**, 27–40.
30 L. Mazutis, J. Gilbert, W. L. Ung, D. A. Weitz, A. D. Griffiths and J. A. Heyman, *Nat. Protoc.*, 2013, **8**, 870–891.
31 A. Cavalli, M. Musterd and F. Mugele, *Phys. Rev. E: Stat., Nonlinear, Soft Matter Phys.*, 2015, **91**, 023013.

